Analysis of phase shift of surface plasmon polaritons at metallic subwavelength hole arrays*

Li Jiang-Yan(李江艳)[a)†], Qiu Kang-Sheng(邱康生)[b)], and Ma Hai-Qiang(马海强)[c)]

[a)] *School of Physics, Peking University, Beijing* 100871, *China*
[b)] *Laboratory of Optical Physics, Institute of Physics, Chinese Academy of Sciences, Beijing* 100190, *China*
[c)] *Faculty of Science, Beijing University of Posts and Telecommunications, Beijing* 100876, *China*

(Received 29 December 2013; revised manuscript received 18 April 2014; published online 20 August 2014)

We present the transmission spectra of light transmitting a metallic thin film perforated with differently shaped subwavelength hole arrays, which are calculated by a plane-wave-based transfer matrix method. We analyze the transmission peak positions and the phase-shift angles of different surface plasmon polariton (SPP) modes by using the microscopic theoretical model proposed by Haitao Liu and Philippe Lalanne [Liu Haitao and Lalanne Philippe 2008 *Nature* **452** 728], in which the phase shift properties of the SPPs scattered by the subwavelength hole arrays are considered. The results show that the transmission peak position and the minus phase shift angle of the SPP increase as the hole size increases. On the other hand, the effective dielectric constant of the metallic film can be deduced by the microscopic theoretical model.

Keywords: surface plasmon resonance, phase shift, metallic nanostructure

PACS: 68.47.De, 79.60.Jv, 81.30.Bx **DOI:** 10.1088/1674-1056/23/10/106804

1. Introduction

Surface plasmon polaritons (SPPs) have attracted extensive and intensive attention of many scientists because of their potential application in localized field enhancement,[1–5] photonics, and nanophotonics circuit construction,[6–10] Raman scattering enhancement,[11–15] biochemical sensor,[16–20] and so on. SPP[21] is a collective oscillation of free electrons in a metal film and the magnitude of its wave vector is a little larger than that of the incident light wave vector. SPP can be excited by scattering a single subwavelength hole, which interacts with other subwavelength structure[22] and modulates the propagation behavior of SPP along the metal–dielectric interface. The interaction between light and metal nanostructures has been extensively investigated, both experimentally and numerically.[23–27] Two-dimensional (2D) and one-dimensional (1D) periodical metallic nanostructures can support SPP at their surface by offering reciprocal lattice vectors,[25,26] induce extraordinary optical transmission (EOT),[28–30] and the strong enhancement of local field.[2] Therefore, periodical metallic nanostructures have extensive applications in building photonics and nanophotonics circuits,[6] field enhancement devices,[2] and biosensor devices,[17] etc.

However, there is little difference between the SPP properties given by the rigorous theoretical method and those obtained from the simple surface plasmon model. In 2008, Liu and Lalanne proposed the microscopic surface plasmon model and achieved surface plasmon results that were in better agreement with the results simulated by rigorous theoretical method.[31] Meanwhile, the concept of phase shift angle was proposed in the microscopic surface plasmon model,[32] which results from scattering of SPP by microstructures and which is associated with shape, size, and other structure parameters.

In this paper, simulated transmission spectra of periodic circular and square hole array by the plane-wave-based transfer matrix method (PWTMM) are presented.[33,34] The microstructured period considered is 0.5 μm in width, 1.0 μm in length, 100 nm in thickness, and the structure size is variable. The transmission peak position and the minus phase shift angle of SPP are discussed by comparing the simple surface plasmon model and the microscopic surface plasmon model.[31] The results show that the minus phase shift angle of SPP changes with the structure parameters, such as array period and hole size. The transmission peak position and the minus phase shift angle of SPP increase as hole size increases. Meanwhile, we can also deduce the effective dielectric constant of the metallic film by using the microscopic surface plasmon model.[31] These results will help us to realize the phase shift relation of the surface plasmon polariton, and present the surface plasmon polariton propagating at the metal–dielectric interface more precisely.

The rest of this paper is arranged as follows. In Section 2, we present the transmission spectrum results of periodic circular and square hole arrays and phase shift results simulated by the microscopic surface plasmon model.[31] In Section 3,

*Project supported by the National Basic Research Program of China (Grant No. 2010CB23202) and the National Natural Science Foundation of China (Grant No. 10805006).

†Corresponding author. E-mail: yanr163@163.com

© 2014 Chinese Physical Society and IOP Publishing Ltd

we further discuss the phase shift properties of the microstructures. Finally in Section 4, we draw some conclusions from the present studies in this paper.

2. Results for circular and square hole arrays

The transmission spectra of periodic nanostructures are simulated by using PWTMM. The film thickness is set to be about 0.1 μm and the periods of periodic circular and square hole array are 0.5 μm and 1.0 μm, respectively. Meanwhile, the geometric size of these nanostructures is also changeable; for instance, the circular hole radius is changed from 0.10 μm to 0.25 μm, the square hole radius is changed from 0.40 μm to 0.50 μm. In the simulation, the dispersion of gold[32] is fully accounted for and the structural symmetry is fully exploited to reduce the computational burden.[33] For the circular and square hole array samples, the system has a two-fold mirror-reflection symmetry. The unknown plane-wave coefficients, which are the important quantities considered in PWTMM, along different crystalline directions, have an intrinsic and definite correlation. As a result, the unknown variables can be reduced four-fold and this significantly reduces the computation time and memory requirement[33] of the computer. We exploit 21×21 plane wave numbers in the simulation. We also test the convergence of numerical simulations by simulating a plane-wave number changed from $21 \times 21 = 441$ to $27 \times 27 = 729$, and the overall spectra. In particular, the major features, such as the transmission peaks of different orders, only change slightly. This means that a good convergence has been achieved.

The transmission spectra of periodic circular hole arrays with period 0.5 μm and 1.0 μm are shown in Fig. 1. Each of the transmission spectra exhibits several orders of transmission peaks and dips.[30] These results are consistent with those in the earlier literature,[31,35,36] and the transmission intensities change is greater as the circular hole radius increases. The lattice constant has a dominant effect on the wavelengths of the transmission peaks and dips, while the hole radius also has some, but far weaker, effects.[36] The transmission enhancement and suppression for the periodic circular hole arrays with hole radius 0.24 μm and the period 0.5 μm, are at 850 nm and 790 nm, corresponding to the SPPs (10) mode at the SiO_2/Au interface, at 660 nm and 615 nm, corresponding to the SPPs (11) mode at the air/Au interface, and at 590 nm and 560 nm, corresponding to the SPPs (10) mode at the air/Au interface. The transmission enhancement and suppression for the periodic circular hole arrays with the hole radius 0.24 μm and the period 1.0 μm, are at 1590 nm and 1515 nm, corresponding to the SPPs (10) mode at the SiO_2/Au interface, at 1180 nm and 1080 nm, corresponding to the SPPs (11) mode at the air/Au interface, and at 1045 nm and 1010 nm, corresponding to the SPPs (10) mode at the air/Au interface.

The transmission enhancement through the subwavelength hole arrays is associated with excitation of SPP. In the simple surface plasmon model, the excitation of SPP mode must satisfy the momentum conservation relation and energy conservation relation at metal film surface,[25,28] which are expressed as

$$\boldsymbol{k}_{\mathrm{sp}} = \boldsymbol{k}_{0\parallel} + i\boldsymbol{G}_x + j\boldsymbol{G}_y, \tag{1}$$

$$\boldsymbol{k}_{\mathrm{sp}} = \left|\boldsymbol{k}_{\mathrm{sp}}\right| = \mathrm{Re}\left(\frac{\omega}{c}\sqrt{\frac{\varepsilon_{\mathrm{m}}(\omega)\varepsilon_{\mathrm{d}}}{\varepsilon_{\mathrm{m}}(\omega)+\varepsilon_{\mathrm{d}}}}\right), \tag{2}$$

where $\boldsymbol{k}_{\mathrm{sp}}$ is the wave vector of SPPs, $\boldsymbol{k}_{0\parallel}$ is the parallel component of the incident light wave vector, $\boldsymbol{G}_x$ and $\boldsymbol{G}_y$ represent the reciprocal vectors of the periodic arrays in the x and y directions, respectively, i and j are integers, $\varepsilon_{\mathrm{m}}(\omega)$ and ε_{d} are the dielectric constants for gold and the substrate material (air or silica), respectively. In the infrared wavelength considered in our simulations, $\varepsilon_{\mathrm{m}}(\omega)$ has a very large negative real part. Consequently, $\boldsymbol{k}_{\mathrm{sp}}$ is larger than, but close to, the wave vector for light in air.

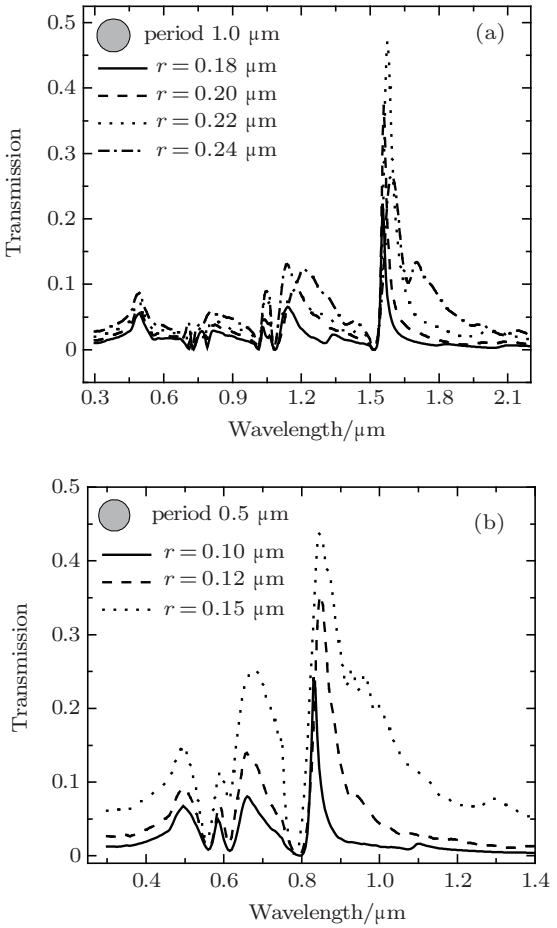


Fig. 1. Simulated transmission spectra of circular hole arrays (a) with the period being 1.0 μm and the hole radius changing from 0.18 μm to 0.24 μm and (b) with the period being 0.5 μm and the radius changing from 0.10 μm to 0.15 μm.

The positions of transmission peaks simulated by the simple surface plasmon model, which originate from the excita-

tion of SPP from Eqs. (1) and (2), are given as follows:

$$\lambda_{\text{peak}} = \lambda_{\text{sp}} = \text{Re}\left[\sqrt{\frac{\varepsilon_{\text{m}}(\omega)\varepsilon_{\text{d}}}{\varepsilon_{\text{m}}(\omega)+\varepsilon_{\text{d}}}}\right] \times \frac{a}{|ix+jy|}, \quad (3)$$

$$\lambda_{\text{dip}} = \lambda_{\text{wood}} = \sqrt{\varepsilon_{\text{d}}}a, \quad (4)$$

where λ_{dip} is the wavelength corresponding to the anomaly in the transmission spectrum. From Eqs. (3) and (4), we can achieve the positions of the transmission enhancement and the adjacent transmission suppression. For instance, the transmission enhancement and transmission suppression positions for the circular hole array with period 0.5 μm and hole radius 0.18 μm are, respectively, at about 793.53 nm and 750 nm, corresponding to the SPPs (10) mode at the SiO_2/Au interface. The difference between the transmission enhancement and transmission suppression is about 43.53 nm, while the value is about 40 nm extracted from the simulated transmission spectrum results shown in Fig. 1. Therefore, we can find that the position difference simulated by the simple surface plasmon model is larger than that by the PWTMM simulated results. Meanwhile, we can find that the difference exists in the transmission anomaly in the transmission spectrum, which shows the insufficiency of the simple surface plasmon model.

Liu and Lalanne proposed the microscopic surface plasmon model[31] to explain the different extraordinary light transmissions through periodic air–hole array and the concept of phase shift angles.[32] According to this model, the modified momentum conservation relation is presented as follows:

$$\boldsymbol{k}_{\text{sp}} = \left|\boldsymbol{k}_{0\parallel} + i\boldsymbol{G}_x + j\boldsymbol{G}_y\right| + \arg(\tau)/a, \quad (5)$$

where $\arg(\tau)$ is the phase shift due to the scattering of nanostructure and the dependence of its magnitude on the detailed geometric parameters of the air holes, such as the hole size and shape.[32] In the case of normal incidence of light, we can directly obtain the wavelength at which SPPs are excited in the gold film perforated with air–hole arrays, which is given as follows:

$$\lambda'_{\text{peak}} = \lambda_{\text{sp}} = \text{Re}\left[\sqrt{\frac{\varepsilon_{\text{m}}(\omega)\varepsilon_{\text{d}}}{\varepsilon_{\text{m}}(\omega)+\varepsilon_{\text{d}}}}\right] \times \frac{a}{|ix+jy|+\arg(\tau)/2\pi}, \quad (6)$$

where a is the lattice constant of periodic hole arrays, i and j are integers. We can obtain the positions of transmission enhancement and the results are more precise than those simulated by the simple surface plasmon model. By comparing Eqs. (3) and (6), we can obtain the phase shift angle of SPP resonant mode and the effect of the phase shift angle on the transmission peak position[32] as follows:

$$\frac{\lambda'_{\text{peak}}}{\lambda_{\text{peak}}} = \frac{1}{1+\dfrac{\arg(\tau)}{2\pi * |n\boldsymbol{x}+m\boldsymbol{y}|}}, \quad (7)$$

$$\arg(\tau) = \left(\frac{\lambda_{\text{peak}}}{\lambda'_{\text{peak}}} - 1\right) * \frac{2\pi}{|n\boldsymbol{x}+m\boldsymbol{y}|}, \quad (8)$$

where n and m are integers, λ'_{peak} and λ_{peak} are the transmission enhancement positions simulated by the microscopic surface plasmon model[31] and the simple surface plasmon model, respectively, $\arg(\tau)$ is the phase shift angle resulting from the scattering of nanostructures, and $\lambda'_{\text{peak}}/\lambda_{\text{peak}}$ is the transmission peak position proportion.[31] In this work, we use the simulated results as the rigorous transmission peak position to examine the phase shift angle.

Figure 2(a) shows the transmission peak position proportions for the circular hole array with period 1.0 μm. When the hole size increases by 60 nm corresponding to the SPP (10) mode at the air/Au interface, the transmission peak position proportion changes from 1.0249 to 1.04. When the hole size increases by 60 nm corresponding to the SPP (11) mode at the air/Au interface, the transmission peak position proportion changes from 1.023 to 1.046. When the hole size increases by 60 nm corresponding to the SPP (10) mode at the SiO_2/Au interface, the transmission peak position proportion changes from 1.06 to 1.098. Meanwhile, as shown in Fig. 2(b), the transmission peak position proportion changes from 1.163 to 1.173 when the hole size increases by 50 nm for the circular hole array with period 0.5 μm, corresponding to the SPP (10) mode at the air/Au interface. The transmission peak position proportion changes from 1.22 to 1.26 when the hole size increases by 50 nm for the circular hole array with period 0.5 μm, corresponding to the SPP (11) mode at the air/Au interface. The transmission peak position proportion changes from 1.05 to 1.07 when the hole size increases by 50 nm for the circular hole array with period 0.5 μm, corresponding to the SPPs (10) mode at the SiO_2/Au interface. We can obtain a conclusion that the transmission peak position proportion increases as the hole radius increases. In comparison, the lattice constant has a more obvious influence than the circular hole radius, which accords with the previous results.[28,35,36] For example, the transmission peak position proportion of the circular hole array with period 1.0 μm is about 1.03, corresponding to the SPP (10) mode at the air/Au interface, while the transmission peak position proportion of the circular hole array with period 0.5 μm is about 1.16, corresponding to the SPP (10) mode at the air/Au interface. The transmission peak position proportions are all larger than 1.0, which shows that the transmission peak positions simulated by the microscopic surface plasmon model[31] are red-shifted apparently and the shifted levels are affected by the nanostructure parameters. Therefore, the scattering effect of the nanostructure induces the surface plasmon resonant position to increase.

The minus phase shift angles of the periodic circular hole array simulated by the microscopic surface plasmon model[32]

are shown in Figs. 2(c) and 2(d). Meanwhile, we can obtain that the minus phase shift angle of the hole array with period 1.0 μm changes from 8.73° to 13.78° corresponding to the SPP (10) mode at the air/Au interface. Meanwhile, the minus phase shift angle of the hole array with period 0.5 μm changes from 50.46° to 53.08°, corresponding to the SPPs (10) mode at the air/Au interface. The minus phase shift angle increases with the circular hole radius increase for the periodic circular hole array with the same period. On the one hand, we can obtain that the lattice constant has two-fold effects on the SPP and more effects on the phase shift angle of SPP. On the other hand, the SPP scattered by the adjacent hole can interact with each other and the period has a stronger effect on the interference of the adjacent SPP.

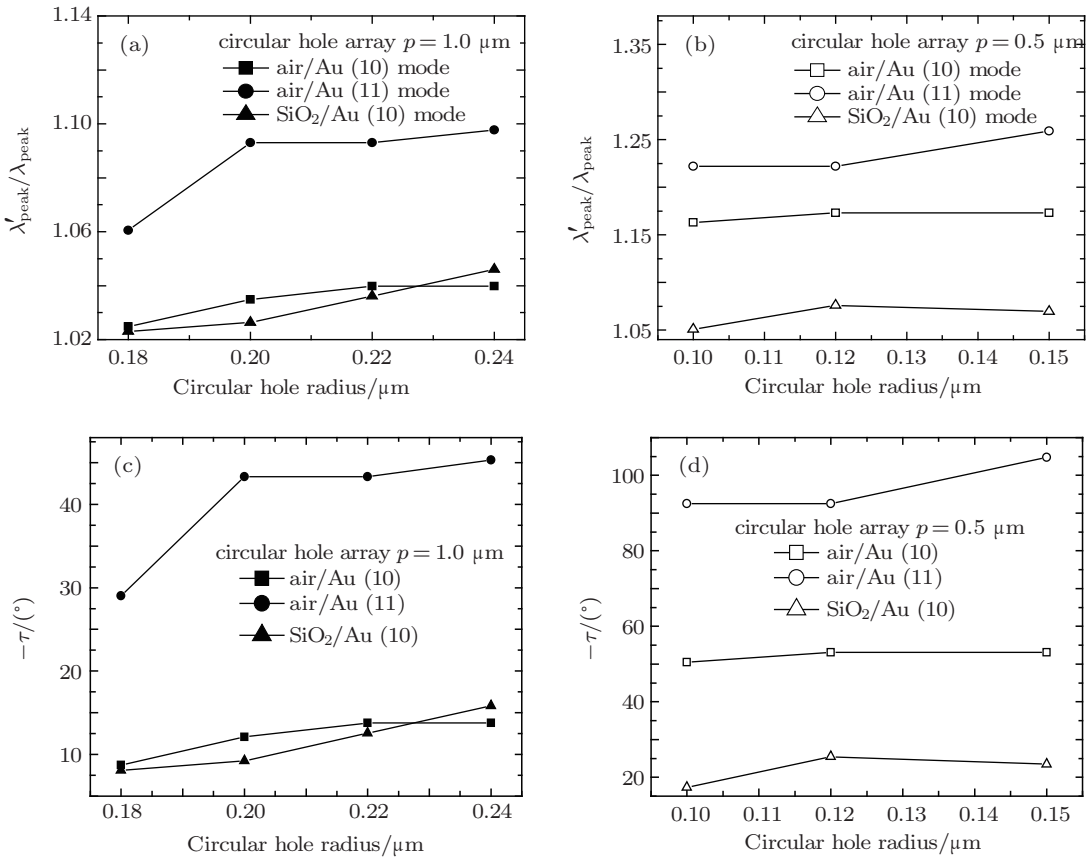


Fig. 2. Simulated transmission peak position proportion of circular hole arrays with the periods of 1.0 μm (a) and 0.5 μm (b); simulated minus phase shift angle of circular hole arrays with the periods of 1.0 μm (c) and 0.5 μm (d).

The transmission spectra of periodic square hole arrays are shown in Fig. 3. The periods of the periodic square hole array are 0.5 μm and 1.0 μm, respectively, and the square hole size changes from 0.4 μm to 2.0 μm. The transmission spectra exhibit several orders of transmission peaks and dips.[30] These results are consistent with those in the earlier literature[25] and the transmission intensities increase with the square hole radius increase. The lattice constant has a dominant effect on the wavelengths of the transmission peaks and dips, while the square hole size also has a certain but far weaker effect. The transmission enhancement and suppression for the periodic square hole arrays with the period 1.0 μm and the square hole size 0.42 μm, are at 1585 nm and 1515 nm, corresponding to the SPP (10) mode at the SiO_2/Au interface. The transmission enhancement and suppression for the periodic square hole arrays with period 0.5 μm and the square hole size 0.42 μm are at 840 nm and 795 nm, corresponding to the SPP (10) mode at the SiO_2/Au interface.

The simulated position difference of transmission enhancement and transmission suppression for SPP is larger than that simulated by the simple surface plasmon model as shown in Fig. 3. According to the microscopic surface plasmon model,[31] we can obtain the transmission peak position proportion and the phase shift angle of the square hole array as shown in Fig. 4. The transmission peak position proportions of the square hole array with the period 1.0 μm and hole size changed from 0.40 μm to 0.50 μm are shown in Fig. 4(a). The transmission peak position proportion changes from 1.0547 to 1.055 when the hole size increases by 100 nm for the square hole array with period 1.0 μm, corresponding to the SPP (10) mode at the air/Au interface. The transmission peak position proportion changes from 1.163 to 1.163 when the hole size increases by 40 nm for the square hole array with period 0.5 μm, corresponding to the SPP (10) mode at the air/Au interface.

The transmission peak position proportions are all larger than 1.0 in Figs. 4(a) and 4(b). The transmission peak positions simulated by the microscopic surface plasmon model[31] are redshifted compared with those simulated by the simple surface plasmon model and the shift levels are affected by the nanostructure parameters, such as the array period and hole size. Meanwhile, we can draw a conclusion that the transmission peak position proportion increases as hole size increases. In comparison, the lattice constant has a more obvious effect than the square hole size, which accords with the previous result.[25] For example, the transmission peak position proportion of the square hole array with period 1.0 μm is about 1.074, corresponding to the SPP (10) mode at the air/Au interface, while the transmission peak position proportion of the circular hole array with period 0.5 μm is about 1.163, corresponding to the SPP (10) mode at the air/Au interface. In conclusion, the scattering effect of the nanostructure induces the SPP position increase.

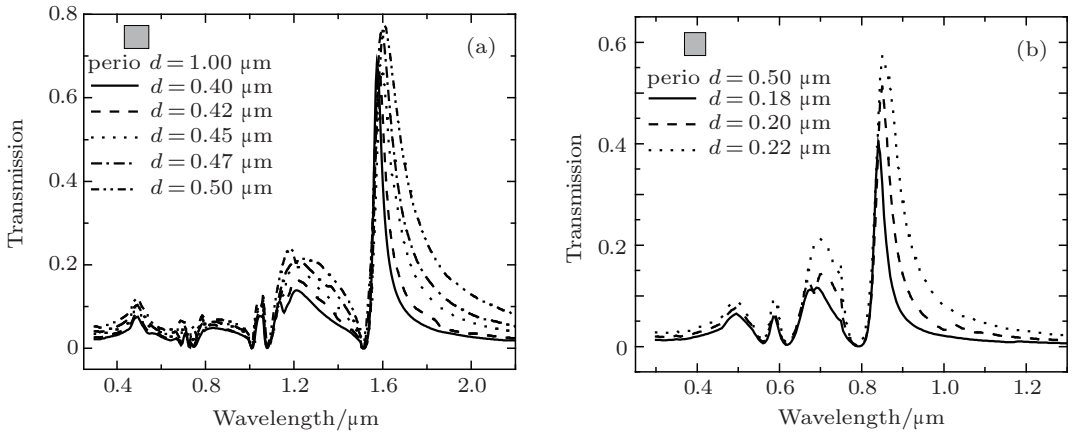


Fig. 3. (a) Simulated transmission spectra of circular hole arrays with the period being 1.0 μm and the hole size changing from 0.40 μm to 0.5 μm, and (b) simulated transmission spectra of square hole arrays with the period being 0.5 μm and the radius changing from 0.18 μm to 0.22 μm.

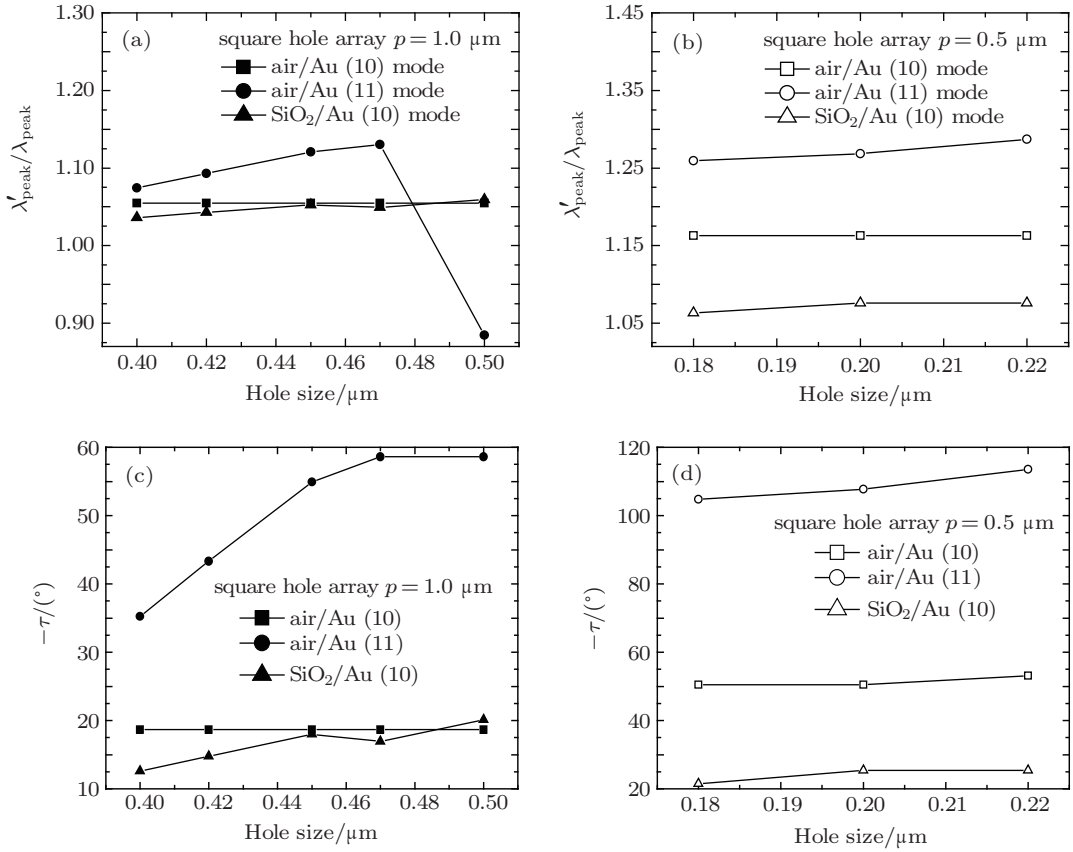


Fig. 4. Simulated minus phase shift angles of the periodic square hole arrays with the periods of 0.5 μm and 1.0 μm, respectively, by the microscopic surface plasmon model. Panel (a) is for the simulated transmission peak proportion of square hole array with the period 1.0 μm, panel (b) for the simulated transmission peak proportion of square hole array with the period 0.5 μm, panel (c) for the simulated minus phase shift angle of square hole arrays with the period 1.0 μm, and panel (d) for the simulated minus phase shift angle of square hole arrays with the period 0.5 μm.

The minus phase shift angle changes from 18.675° to 18.685° when the hole size increases by 100 nm for the periodic square hole array with period 1.0 μm, corresponding to the SPP (10) mode at the air/Au interface. Meanwhile, the minus phase shift angle changes from 50.46° to 53.08° when the hole size increases by 40 nm for the periodic square hole array with period 0.5 μm, corresponding to the SPP (10) mode at the air/Au interface. The minus phase shift angle increases with the square hole size increase for the periodic square hole array, and it is larger than that simulated by the simple surface plasmon model without considering the scattering of SPP by the nanostructure. In comparison, the lattice constant has a more obvious effect on minus phase shift angles than the square hole size, which is consistent with the previous result.[25] For example, the minus phase shift angle of the square hole array with period 1.0 μm is about 18.68°, corresponding to the SPP (10) mode at the air/Au interface, while that of the circular hole array with period 0.5 μm is about 50.26°, corresponding to the SPPs (10) mode at the air/Au interface. Meanwhile, the minus phase shift angle reflects the scattering effect of the nanostructure, which is affected by the nanostructure parameters, such as structure period and hole size. The minus phase shift angle of the square hole array is a little larger than that of the circular hole array, which shows that the scattering effect of the square hole is a little larger than that of the circular hole array.

The existence of the minus phase shift angle shows the effect of the nanostructure on the SPP, which induces the change of the SPP phase. Meanwhile, the above results are consistent with previous results[25] and we also simulate the near field intensity distribution to observe the scattering effect of the nanostructure by the finite element methods, which is supplied by the Comsol Corporation. The result is shown in Fig. 5. We can clearly observe the resonant wave excited by the nanostructure shown in Figs. 5(a) and 5(c). Meanwhile, the near-field intensity profile shows the SPP propagation away from the circular hole center, which is quite different from the results simulated by the simple surface plasmon model from the field intensity profiles in Figs. 5(c) and 5(d). The results show the existence of the SPP phase shift scattered by the nanostructure and the corresponding resonant wave.

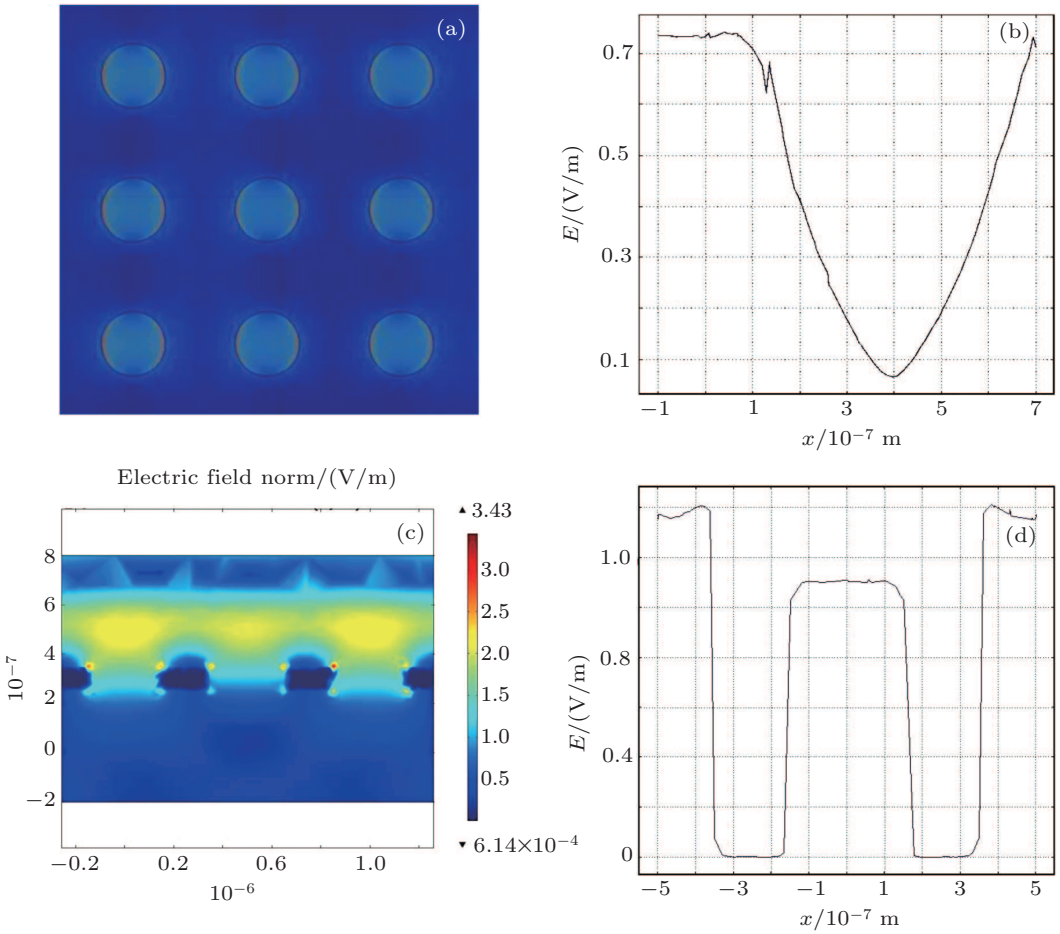


Fig. 5. (color online) Field intensity distributions of the periodic circular hole array with periods of 1.0 μm and 0.5 μm, simulated by the finite element methods. Panel (a) is for the near field intensity for the periodic circular hole array, with the period 1.0 μm and the hole radius 0.24 μm at the wavelength 1590 nm. Panel (b) is for the near-field intensity profile for the periodic circular hole array, with the period 1.0 μm and the hole radius 0.24 μm at the wavelength 1590 nm. Panel (c) is for the near-field intensity for the periodic circular hole array, with the period 0.5 μm and the hole radius 0.15 μm at the wavelength 0.845 μm. Panel (d) is for the near-field intensity profile for the periodic circular hole array, with the period 0.5 μm and the hole radius 0.845 μm.

3. Further discussion

The transmission peak position proportion and the minus phase shift angle increase with the period and the hole size increase. The phase shift angle reflects the scattering effect of the nanostructure and it is affected by the hole size and other structure parameters. We can deduce the effective dielectric constant equation of the periodic nanostructure from the microscopic surface plasmon model and the simple surface plasmon model according to Eqs. (2) and (3), when the light is incident with an incident angle of 0°,

$$\varepsilon_{\text{meff}} = \frac{g\varepsilon_{\text{g}}}{\varepsilon_{\text{g}} - g}, \tag{9}$$

$$g = \left(\frac{2\pi c}{w\lambda_{\text{spp}}}\right)^2 = \left(\frac{\lambda_0}{\lambda_{\text{spp}}}\right)^2, \tag{10}$$

where $\varepsilon_{\text{meff}}$ is the effective dielectric parameter corresponding to the gold material with periodic hole array, ε_{g} is the dielectric constant of the glass substrate, w and c are the frequency and the light speed in vacuum respectively, and λ_0 and λ_{spp} are the incident light wavelength in air and the surface plasmon wavelength along metal–dielectric interface respectively.

We can deduce the effective dielectric constant of the metal for the periodic circular hole array with the period 1.0 μm and the hole radius 0.18 μm, corresponding to the SPP (10) mode at the air/Au interface. We can deduce that the minus phase shift angle is about 8.737° and the surface plasmon wavelength is 1.02487μm. The effective dielectric constant is about −101 for the metal film with periodic circular hole array according to Eqs. (9) and (10). This means that we can achieve the effective dielectric constant of metal film with the periodic hole array and it can be used to directly simulate the transmission spectrum and field intensity.

4. Conclusions

In this paper we simulated the transmission spectrum for the periodic hole array by PWTMM. The transmission peak position proportion and the minus phase shift angle are achieved by comparing the microscopic surface plasmon model and the simple surface plasmon model. The transmission peak position proportion and the minus phase shift angle increase as the hole size increases, and the lattice constant has a stronger effect on transmission peak position proportion and minus phase shift. In view of the minus phase shift angles reflecting the scattering effect of the nanostructure, the scattering effect of the square hole is larger than that of the circular hole array. Meanwhile, we can further observe the scattering effect of the microstructures and the change of surface plasmon polariton.

References

[1] Gresillon S, Aigouy L, Boccara A C, Rivoal J C, Quelin X, Desmarest C and Gadenne P 1999 *Phys. Rev. Lett.* **82** 4520
[2] Hu B, Liu J, Gu B Y, Di S, Sun X D and Wang S Q 2007 *J. Opt. Soc. Am. A* **24** 1084A1
[3] Zayats A V and Smolyaninov Igor I 2003 *J. Opt. A: Pure Appl. Opt.* **5** S16
[4] Tanaka Kazuo and Tanaka Masahiro 2004 *J. Opt. Soc. Am. A* **21** 2344
[5] Onuta Tiberiu-Dan, Waegele Matthias, DuFort Christopher C, Schaich Willianm L and Dragnea Bogdan 2007 *Nano Lett.* **7** 557
[6] Luo Xianggang and Ishihara Teruya 2004 *Appl. Phys. Lett.* **84** 4780
[7] Berini P, Charbonneau R, Lahoun N and Mattiussi G 2005 *J. Appl. Phys.* **98** 043109
[8] Yin Leilei, Valsko-Vlasov Vitali K, Pearson John, Hiller Jon M, Hua Jiong, Welp Ulrich, Brown Dennis E and Kimball Clyde W 2005 *Nano Lett.* **5** 1399
[9] Fang Nicholas, Lee Hyesog, Sun Cheng and Zhang Xiang 2005 *Science* **308** 534
[10] Ozbay Ekmel 2006 *Science* **311** 189
[11] Jackel F, Kinkhabwala A A and Moerner W E 2007 *Chem. Phys. Lett.* **446** 339
[12] Felidj N, Aubard J, Levi G, Krenn J R, Salerno M, Schider G, Lamprecht B, Leitner A and Aussenegg F R 2002 *Phys. Rev. B* **65** 075419
[13] Laurent Guillarme, Felidj Nordin, Grand Johan, Aubard Jean, Levi Georges, Hohenar Andreas, Aussenegg Frantz R and Krenn Joachim R 2006 *Phys. Rev. B* **73** 245417
[14] Gunnarsson L, Bjerneld E J, Petronis H Xu, Petronis S, Kasemo B and Kall M 2001 *Appl. Phys. Lett.* **78** 802
[15] Haes Amanda J, Zou Shengli, Zhao Jing, Schatz George C and Duyne Richard P Van Duyne 2006 *J. Am. Chem, Soc.* **128** 10905
[16] Guo H C, Nau D, Radke A, Zhang X P, Stodolka J, Yang X L, Tikhodeev S G, Gippius N A and Giessen H 2005 *Appl. Phys. B* **81** 271
[17] Olofsson Linda, Rindzevicius Tomas, Pfeiffer Indriati, Kall Mikael and Hook Fredic 2003 *Langmuir* **19** 10414
[18] Nelson Bryce P, Grimsrud Timothy E, Liles Mark R, Goodman Robert M and Corn Robert M 2001 *Anal. Chem.* **73** 1
[19] Okamoto Takayuki, Yamaguchi Ichirou and Kobayashi Tetsushi 2000 *Opt. Lett.* **25** 372
[20] Haes Amanda J, Zou Shengli, Schatz George C and Van Duyne Richard P 2004 *J. Phys. Chem. B* **108** 6961
[21] Ebbesen T W, Lezec H J, Ghaemi H F, Thio T and Wolff P A 1998 *Nature* **391** 667
[22] Yin L, Vlasko-vlasov V K, Rydh A, Pearson J, Welp U, Chang S H, Gray S K, Schatz G C, Brown D B and Kimball C Wl 2004 *Appl. Phys. Lett.* **85** 467
[23] Aigouy L, Lalanne P, Hugonin J P, Julie G, Mathet V and Mortier M 2007 *Phys. Rev. Lett.* **98** 153902-1
[24] Schouten H F, Kuzmin N, Dubois G, Visser T D, Gbur G, Alkemade P F A, Blok H, Hooft G W't, Lenstra D and Eliel E R 2005 *Phys. Rev. Lett.* **94** 053901
[25] Kwak Eun-Soo, Henzie Joel, Chang Shih-Hui, Gray Stephen K, Schatz George C and Odom Teri W 2005 *Nano Lett.* **5** 1963
[26] Tetz Kevin A, Rokitski Rostislav, Nezhad Maziar and Fainman Yeshaiahu 2005 *Appl. Phys. Lett.* **86** 111110
[27] Altewischer E, van Exter M P and Woerdman J P 2002 *Nature* **418** 304
[28] Sun M, Liu R J, Li Z Y, Cheng B Y, Zhang D Z, Yang H F and Jin A Z 2006 *Chin. Phys.* **15** 1591
[29] Przybilla F, Genet C and Ebbesen T W 2006 *Appl. Phys. Lett.* **89** 121115
[30] Ckark A W, Sheridan A K, Glidle A, Cumming D R S and Cooper J M 2007 *Appl. Phys. Lett.* **91** 093109
[31] Liu Haitao and Lalanne Philippe 2008 *Nature* **452** 728
[32] Palik E D 1985 *Handbook of Optical Constant of Solids* (Orlando: Academic Press)
[33] Li Z Y and Ho K M 2003 *Phys. Rev. B* **68** 245117
[34] Li Z Y and Ho K M 2003 *Phys. Rev. B* **67** 165104
[35] Li J Y, Li Z Y, Yang H F and Jin A Z 2008 *J. Appl. Phys.* **104** 114303
[36] Li J Y, Hua Y L, Fu J X and Li Z Y 2010 *J. Appl. Phys.* **107** 073101